Bulletin of Geophysics and Oceanography Vol. 67, n. 1, pp. 19-40; March 2026
DOI 10.4430/bgo00502

The assessment of traffic-induced vibrations in urban areas by means of cost-effective sensors: a case study for a historic building in Trieste, north-eastern Italy

G. Capotosti, L. Cataldi, D. Ertuncay, C. Scaini and V. Poggi

National Institute of Oceanography and Applied Geophysics - OGS, Trieste, Italy

(Received: 27 March 2025; accepted: 2 August 2025; published online: 14 January 2026)

ABSTRACT Traffic-induced vibrations represent a problem in urban areas where repeated dynamic loading from heavy vehicles can affect both the structural integrity of buildings and occupant comfort. This study addresses the dynamic response of a historic masonry building in the Borgo Teresiano district of Trieste, a site with Quaternary sediments known to amplify ground motions due to their low stiffness and heterogeneity. The aim was to investigate the interaction between traffic-induced ground motion and the structure's response by using a rapid, non-invasive monitoring approach. During a short-term campaign, low-cost seismic stations with triaxial velocimeters were installed at the base and top of the structure. Ambient vibration data were analysed using: i) Fourier amplitude spectra combined with the rotation of horizontal components, ii) spectral ratios between sensor pairs within the structure to identify main structural modes and amplification directions, iii) single station horizontal-to-vertical spectral ratio analysis to identify fundamental soil resonance frequency. The results showed a resonance peak at 11 Hz in the vertical component at the top floor, interpreted as responsible for the amplification of vibrations caused by repeated traffic combined with soil-structure interaction, with levels exceeding discomfort thresholds and impacting wellbeing. This highlights how cost-effective sensors and ambient noise analysis support mitigation strategies.

Key words: cost-effective sensors, traffic-induced vibrations, site effects, seismic noise, historic buildings.

1. Introduction

Building vibrations caused by road traffic, especially by trucks and buses, are becoming an increasingly important issue due to the increasing vehicle load and volume of road traffic itself (Hao *et al.*, 2001). These vibrations are caused by the interaction between the vehicle wheels and the unevenness of the road surface and can propagate through the ground to adjacent structures. Under certain conditions, such vibrations can reach amplitudes that can cause damage to residential and historical buildings (Crispino and D'Apuzzo, 2001; Bongiovanni *et al.*, 2011; Beben *et al.*, 2022). Beyond the structural effects, traffic-induced vibration can affect the comfort and quality of life of neighbouring residents, causing nuisance or, in some cases, health problems (Woodcock *et al.*, 2012; Sica *et al.*, 2014; Waddington *et al.*, 2014). The characteristics of traffic-induced vibration depend on several interrelated factors, including vehicle type and speed, road conditions, suspension systems, subsoil properties, and building dynamics (Erkal

et al., 2010). Unevenness of the road surface has been shown to significantly amplify vibration levels (Al-Hunaidi *et al.*, 1995) and the type of vehicle suspension can also strongly influence the frequency content and amplitude of transmitted vibrations (Hunaidi *et al.*, 2000). Furthermore, the predominant frequencies and amplitudes are largely controlled by the mechanical and geometrical properties of the soil and building (Erkal *et al.*, 2010). Various mitigation strategies have been proposed, such as modifying the structural properties of the building through changes in damping or stiffness (Pridham *et al.*, 2021) or modifying the road pavement using vibration-attenuating layers (Costanzo *et al.*, 2022a). Adjustments to traffic flow or vehicle types have also been considered (Hunaidi *et al.*, 2000). However, before effective measures can be taken, a detailed assessment of the sources and intensity of the vibrations is required. These assessments need to be compared with national or international guidelines (ISO, 2003; BSI, 2008; ANC, 2012) to evaluate their potential impact. Nevertheless, there is still no consensus on appropriate descriptors for social exposure, and robust exposure-response models require empirical data to be collected efficiently and consistently (Sica *et al.*, 2014). In recent decades, research on traffic-induced vibrations has made considerable progress through the use of analytical modelling, field experiments, and hybrid approaches. Kouroussis *et al.* (2011) conducted extensive research on road and rail traffic-induced vibration employing numerical simulations validated against field measurements. Their studies emphasise the need to include traffic parameters and soil structure interaction effects in prediction models. Caballol *et al.* (2022) provided a critical overview of the effects of traffic vibration on urban structures and highlighted the limitations of current modelling techniques and the need for harmonised mitigation standards. Recently, ambient vibration measurement techniques have emerged as a cost-effective and non-invasive method to assess the dynamic behaviour of buildings. For instance, Lopes *et al.* (2016) successfully applied ambient vibration analysis to identify the fundamental frequencies of traffic-exposed buildings in Portugal. Zhang *et al.* (2019) demonstrated how ambient vibration data can be integrated with other geophysical methods to improve the interpretation of traffic-induced signals in building systems. The advent of low-cost sensors, particularly micro-electro-mechanical systems (MEMS) sensor-based accelerometers, has significantly improved the feasibility of large-scale monitoring (Bragato *et al.*, 2025). These devices have been shown to be suitable for detecting traffic-induced vibrations in both high- and low-income urban areas (Rivas *et al.*, 2012; Shiferaw, 2021), as they are affordable, portable, and easy to deploy. Furthermore, Celebi (2000) emphasised the importance of permanent structural monitoring of critical infrastructures and advocated the use of continuous measurement devices to assess the impact of traffic and seismic effects over time.

In the Italian context, several studies have addressed the vulnerability of urban structures to traffic-induced vibrations, with particular attention to historic buildings. Mucciarelli and Gallipoli (2007) and Gallipoli *et al.* (2009, 2023) have demonstrated the effectiveness of ambient noise techniques to determine the dynamic properties of soils and buildings. Bongiovanni *et al.* (2011) and Sica *et al.* (2014) integrated engineering vibration measurements with community surveys to assess both physical and social impacts. More recent applications include the use of low-cost velocimeters for traffic vibration assessment (Costanzo *et al.*, 2022a), the use of advanced remote sensing tools such as laser scanning (Costanzo *et al.*, 2022b), and image processing (Mugnai *et al.*, 2022) to monitor structural response. In addition, Ertuncay *et al.* (2024) proposed a signal processing method capable of distinguishing between vehicle-induced and earthquake-induced vibrations, contributing to the advancement of source detection techniques in Italian seismic and urban monitoring networks. Currently, the most common methods for studying traffic-induced vibrations include both remote sensing and direct measurements with high-resolution or low-cost instruments (Erkal *et al.*, 2020). Ambient vibration measurement

techniques are particularly suitable for preliminary investigation as they provide a rapid and non-invasive approach to evaluate the resonance properties of buildings and subsoils (Mucciarelli and Gallipoli, 2007; Gallipoli *et al.*, 2009; Guillier *et al.*, 2016). While high-sensitivity broadband seismometers offer detailed spectral analyses, their use is often limited by logistical constraints and cost. In contrast, low-cost MEMS-based accelerometers enable wide-area surveys and short-term monitoring campaigns and facilitate the identification of vibration peaks related to both ambient noise and building dynamics (Scaini *et al.* 2021; Gallipoli *et al.* 2023; Petrovic *et al.*, 2023). The development of accessible and reliable methods for the assessment of traffic-induced vibration is crucial not only for the identification and mitigation of adverse effects, but also for the calibration of exposure response models (Woodcock *et al.*, 2012; Sica *et al.*, 2014). Despite their demonstrated potential, cost-effective measurement methods are still underutilised in real urban scenarios due to practical limitations among which the need to access private buildings.

This paper presents the results of a monitoring campaign carried out on a residential building located in the Borgo Teresiano district of Trieste (north-eastern Italy), selected based on repeated complaints about traffic-induced vibrations. The study was carried out using a lightweight and cost-effective instrumental setup to measure ambient vibrations both in the building and the underlying subsoil. The aim of the study is to assess the feasibility of using low-cost seismic stations for a rapid identification of the dynamic characteristics of buildings and of the predominant sources of vibration so as to support future mitigation and monitor strategies on an urban scale.

2. Experimental setup description

2.1. Building description

The building under investigation is located in the heart of the historical district of Borgo Teresiano in Trieste (Fig. 1). The building dates from the second half of the 19th century and is an example of Austro-Hungarian neoclassical architecture typical of the urbanisation period of Borgo Teresiano. The building consists of five floors above ground without underground levels. The structure has an irregular trapezoidal shape with a curved side that adapts to the surrounding road network. Structurally, the building consists of load-bearing masonry made of stone and brick. The floors, made of reinforced concrete, with the exception of the upper floor which is made of wood, provide variable structural rigidity that can influence the transmission of vibrations within the building. The roof is a pitched structure covered with terracotta tiles. The building is constantly exposed to vibrations caused by heavy vehicular traffic as it is located on roads frequently used by buses and trucks. The presence of loosely compacted soils beneath the foundations can exacerbate the transmission of mechanical waves and potentially increase the loads acting on walls and floors. The combination of masonry construction, building geometry, and subsurface geological conditions requires a careful assessment of the structure's dynamic response to both earthquakes and urban traffic-induced vibrations.

2.2. Subsoil characterisation

Borgo Teresiano in Trieste is located in a geologically complex area on the Gulf of Trieste, the northernmost point of the Adriatic basin, where the Trieste Karst rocky plateau meets the coastal strip. The bedrock in this broader area consists of geological formations of different ages,

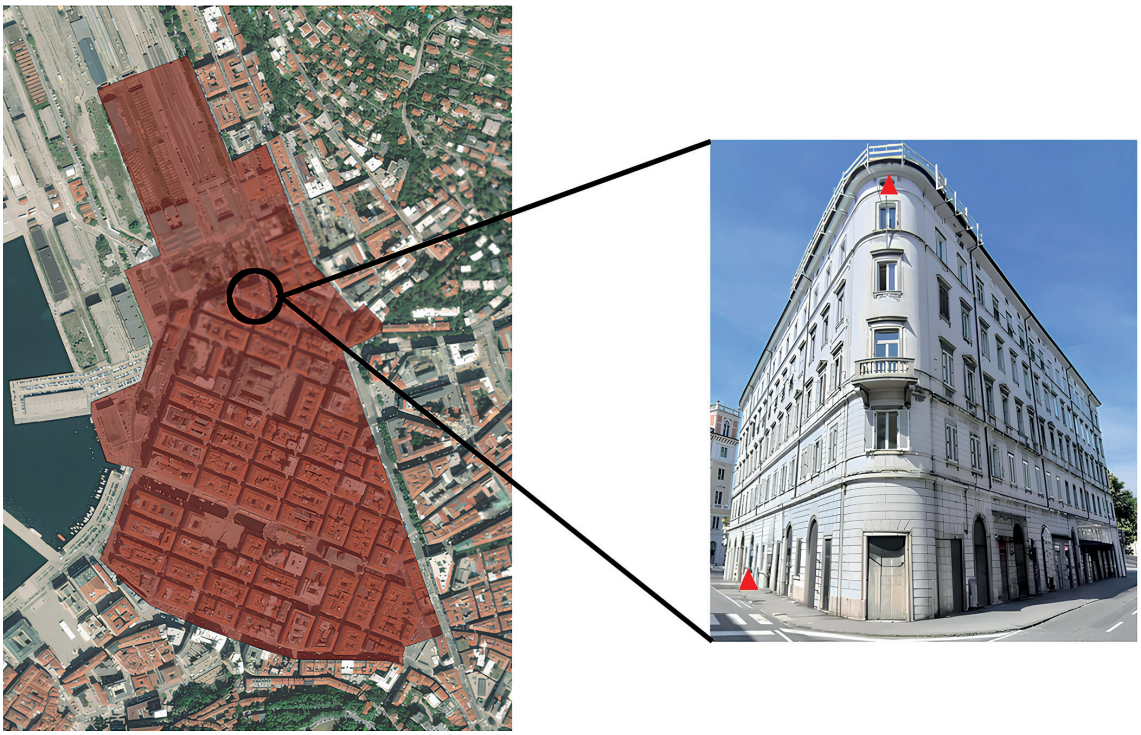

Fig. 1 - Left: aerial view from Google Maps of the area of Borgo Teresiano (marked in red). The black circle marks the location of the building under analysis. Right: a view of the analysed building displaying the position of the base and top stations, marked with red triangles.

ranging from ancient carbonate platforms from the Mesozoic era to the more recent Eocene deposits, characterised by alternating layers of marl and sandstone. Near the coast, where Borgo Teresiano is located, the bedrock is overlain by a mantle of Quaternary deposits, alternating between alluvial and marine origin. These deposits have accumulated over the last 2.6 million years as a result of climate fluctuations and sea-level variations (Busetti *et al.*, 2012). These sediments, which mainly consist of sands, silts, and gravels, are less consolidated than the older rock formations and can significantly modify the propagation of seismic waves, often amplifying ground motion and altering its frequency content. In addition to its geological nature, Borgo Teresiano is characterised by significant human interventions, which have significantly altered the natural composition of the soil (Busetti *et al.*, 2012). Originally a coastal marshland, the district was reclaimed and filled with artificial material from the 18th century onwards. This fill, consisting of unconsolidated sand, gravel, silt, clay, and construction debris, has given the subsoil a heterogeneous composition and variable density. The use of fill materials for urban expansion has further altered the transmission of seismic waves, increasing the susceptibility of some areas to the amplification of ground motion generated by both natural and anthropogenic sources, such as traffic loads.

A classification of the urban area into homogeneous microzones based on seismic behaviour, considering different geological formations and their lithotechnical, geotechnical, and hydrogeological characteristics, is provided by the seismic microzonation study of the city of Trieste (Regione Autonoma Friuli Venezia Giulia – Comune di Trieste, 2016a). This analysis shows that the Quaternary sediments and artificial fillings present in Borgo Teresiano can influence the amplification of seismic waves, affecting the area's response to vibrations. The

map corresponding to the homogeneous microzones in seismic perspective - MOPS (Regione Autonoma Friuli Venezia Giulia – Comune di Trieste, 2016b) classifies Borgo Teresiano within the stable zones susceptible to local amplification (Gordini *et al.*, 2003). Although the area is considered geomechanically stable, the heterogeneous composition of its subsoil can markedly influence seismic wave behaviour. This phenomenon is of particular importance not only for seismic hazard assessment but also for evaluating the effects that heavy vehicular traffic, which can be amplified under certain conditions, induces on vibrations and how these influence the structural response of buildings and infrastructures.

3. Methodology

The vibrational modes of a system (either the soil, a structure, or a combination thereof) represent the characteristic patterns of motion that occurs at its natural frequencies and provide key information for the effective characterisation of motion's dynamic behaviour under seismic loading. The main natural frequencies of the soil-structure system can be determined using conventional non-parametric identification methods (Paolucci, 1993; Meli *et al.*, 1998) based on the comparison of motions recorded at different locations, such as the top and bottom of the building. To effectively highlight the transfer function response of a building, the Fourier amplitude spectrum (*FAS*) of ambient noise measurements recorded at the top of the structure can be normalised by the corresponding *FAS* recorded at the bottom, which is assumed to approximate the free field motion, i.e. the shaking input to which the building is subjected. This approach remains a first-order approximation, due both to the buildings being located in a densely urbanised area where neighbouring buildings influence the input seismic wavefield and to the fact that the structure itself radiates part of the wavefield back into the soil. Since the aim of this study is to perform a preliminary, fast, and simplified modal identification, such an approximation is considered acceptable without having to resort to more complex deconvolution analyses.

Beyond the characterisation of the building response, a passive seismic survey using the horizontal-to-vertical spectral ratio (*HVSR*) method is used to disambiguate the fundamental frequency of the soil itself from that of the soil-structure system. This method, commonly referred to as the Nakamura method (Nakamura, 1989, 1996, 2000), is based on the analysis of the spectral ratio between vertical and horizontal components of the motion and is extensively used to characterise the seismic response of soil deposits based on ambient noise recordings (microtremors). Ambient noise includes a broad spectrum of vibrations that propagate in the ground due to natural phenomena, such as ocean waves, and to anthropogenic activities, such as vehicle traffic which is expected to be predominant in the case at hand. Despite certain limitations posed by the *HVSR* method, especially the fact that by itself it is not sufficient to characterise the absolute values of seismic amplification, this low-cost method has become a widely accepted and valuable tool for estimating the natural frequency of soft soil sites, particularly in the context of microzonation and site response studies. To ensure methodological consistency, the acquisition and interpretation of the HVSR curves were conducted in accordance with the SESAME (Site EffectS Assessment using AMbient Excitations) guidelines (Bard, 2004), which were developed to provide a standardised framework for ambient noise-based investigations. These guidelines, which were developed as part of the SESAME European project (Project No. EVG1-CT-2000-00026), aim to standardise analysis procedures, assess curve reliability by taking into account signal quality, determine resonance frequency of the site, and estimate subsurface depth. Compliance with the SESAME criteria is essential to obtain reliable results in HVSR

surveys. To correctly implement these guidelines, triaxial recordings are required over a wide frequency range (0.1-100 Hz) and with a sufficiently long duration (typically 20-30 minutes). These recordings are, then, processed to derive *HVSR* spectra, which provide information about the subsurface structure and the local seismic response of the site.

3.1. Deployment description

Three measurement locations were selected as the most suitable for evaluating the dynamic behaviour of the structure (Fig. 2): one at the base and one at the top of the building to assess the structural transfer function through standard spectral ratios, and an additional station on the top floor to investigate the influence of the wooden slab, as will be described in more detail later.

Given the structural characteristics of the building and the need to record the low-amplitude signals of ambient noise, compact and cost-effective seismic instruments with high sensitivity and data fidelity were selected. The Lunitek Sentinel Geo seismic station meets these requirements, offering an excellent quality-to-price ratio and being specifically designed for detecting and analysing ground vibrations. This makes it an effective tool for structural monitoring, providing reliable data without compromising measurement accuracy. Its compact and lightweight design further simplifies survey setup and enables rapid deployment in diverse monitoring environments.

Each station is equipped with an embedded triaxial velocimetric sensor consisting of three geophones with a natural frequency of 4.5 Hz. The signals from these geophones are sampled synchronously with a 24-bit resolution, which ensures high data fidelity and a dynamic range exceeding 120 dB. The sampling frequency was set at 250 samples per second to capture a detailed recording of the microtremors. Global positioning system receivers were used to ensure precise time synchronisation for all measurements. For the purpose of this study, velocimeters were selected as the primary sensor for the analysis as they have a higher sensitivity and provide a more detailed and accurate representation of the building's vibration behaviour.

Regarding data collection duration, the seismic station at the base of the building (referred to as 'base station'), powered solely by its internal battery, recorded for approximately six hours before shutting down. In contrast, the station at the top (referred to as 'wall station') was connected to a continuous power supply, enabling nearly two months of uninterrupted acquisition and providing a long-term dataset for structural analysis. The third station, installed

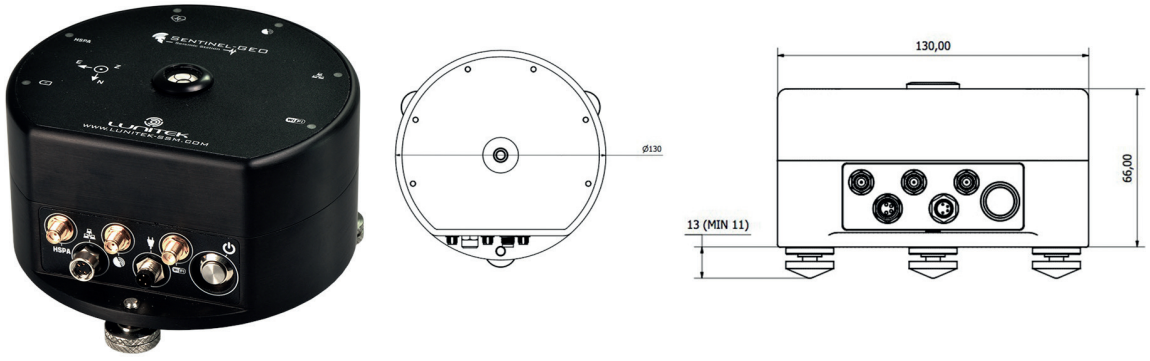

Fig. 2 - Left: an image of the Lunitek Sentinel GEO sensor shows the connections for the GPS, LTE and Wi-Fi antennas, the power supply connection, and the three adjustable feet for correct positioning. Centre: schematic top view with indication of the device diameter (130 mm). Right: side view with the most important overall dimensions, including the total height (66 mm). Technical information and diagrams are sourced from the official Lunitek website, https://lunitek.it/seismic/digital-seismic-sensors/sentinel-geo/.

on the top floor, operated for only about 30 minutes, with the specific aim of evaluating the localised dynamic response of the wooden slab. Despite the short recording time, the acquired data were of sufficient quality for the intended analysis. All data and associated metadata from the three measurement stations, including acquisition parameters and sensor configurations, are available in Capotosti *et al.* (2025).

4. Data processing and results

4.1. Pre-processing

In order to capture the average traffic-induced vibrations of the building, a 25-minute time window, corresponding to the end of the morning rush hour on a typical working day (Table 1), was selected for the data analysis. The raw velocimetric data were elaborated using a standard pre-processing routine consisting of detrending, baseline correction, and complete removal of the instrumental response.

Table 1 - Time intervals used for data analyses at each site.

Station	Start time (UTC)	End time (UTC)
slab	2023-07-27T09:57:30Z	2023-07-27T10:22:30Z
wall	2023-07-27T09:57:30Z	2023-07-27T10:22:30Z
base	2023-05-19T10:55:00Z	2023-05-19T11:20:00Z

Due to the irregular geometry of the building, the seismic signals were originally recorded with horizontal orientation to the east and north directions, as it was not possible to align the sensors with the nearest sides. In order to accurately assess the maximum horizontal vibration of the building in response to the traffic-induced excitation, different rotation angles were tested to identify the preferential directions in which the motion would be amplified. At each measurement location, the horizontal components were rotated by an angle θ that varied in 10-degree increments from 0° to 180° (Fig. 3, left), and the corresponding changes in the mean *FAS* peak values were observed. Each resulting *FAS* represents both the spectrum of the signal rotated by θ (represents the spectrum of the rotated signal) and the spectrum of the signal rotated by θ+180°, since it is an absolute amplitude value.

The resulting variations of the mean *FAS* peak amplitudes at the different locations are displayed in Fig. 4. A consistent maximisation of all peaks at a rotation of θ ~130° can be observed. This is an intermediate value between the directions of alignment, i.e. θ ~170° and θ ~110°, of the sides of the building on which the measurements were made (Fig. 3, right). Although a complete dynamic modelling of the building was beyond the scope of this work, the presence of complex higher vibrational modes at angles not aligned with the walls is compatible with the irregular geometry of the building. Therefore, all analyses were conducted using signals rotated by θ=130°, in order to assess the maximum response of the building to ambient noise excitations.

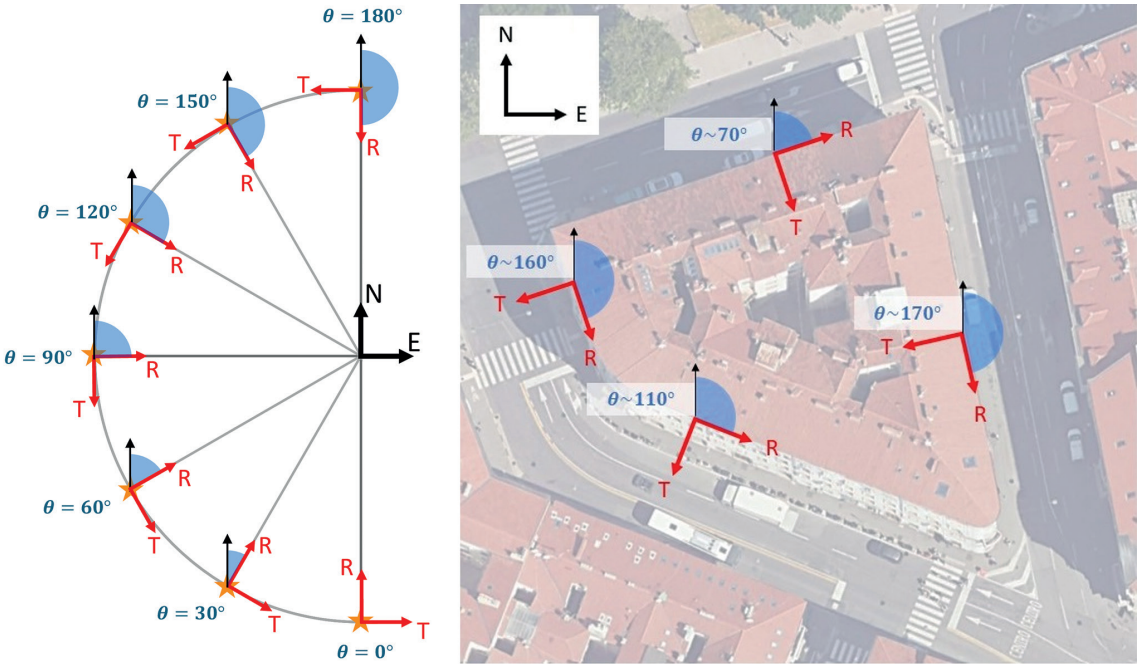

Fig. 3 - Visual representation of the rotation of the signal originally oriented in the NE direction by an arbitrary angle *θ*, into transverse (T) and radial (R) components (left). Corresponding orientation of the walls of the building in which the measurements were carried out (right).

4.2. The Fourier amplitude spectrum and spectral ratios

For each site, the selected 25-minute signal was divided into 20% overlapping windows with 30-second durations. The corresponding *FAS*s were calculated and smoothed according to the Konno-Ohmachi formula (Konno and Ohmachi, 1998), with smoothing coefficient $b = 40$. The mean *FAS* value and the associated variance were, then, estimated using the modified Cox method (Olsson, 2005), which assumes the *FAS* value at each frequency point to be log-normally distributed. For the wall site, an example is displayed in Fig. 5. Here, the individual spectra corresponding to each 30-second window are also represented along with the mean *FAS* and its 95% confidence interval. The resulting mean spectra for each site and for each component are summarised in Fig. 6.

Based on the previously determined mean *FAS*s, the spectral ratio for each component (radial, transverse, and vertical) was calculated as the ratio between the mean *FAS* at two sites. The selected site combinations enable the analysis of the motion of the slab relative to the wall (slab/wall case) and to the base (slab/base case), as well as the motion of the wall relative to the base (wall/base case). The corresponding results are shown in Fig. 7. A peak at 11 Hz is evident in the ratios of the vertical components, while additional peaks at 2.5, 3.8, 5.5, and 7.2 Hz emerge in the ratios made on horizontal components with respect to the base.

4.3. Site analysis

A correct interpretation of the resonance frequencies detected by spectral analysis must also take into account the local seismic response at the site. In this context, the standard *HVSR* method was applied according to the SESAME guidelines (Bard, 2004). This method is based on the analysis of recorded ambient seismic noise with the aim of extracting the spectral ratio between

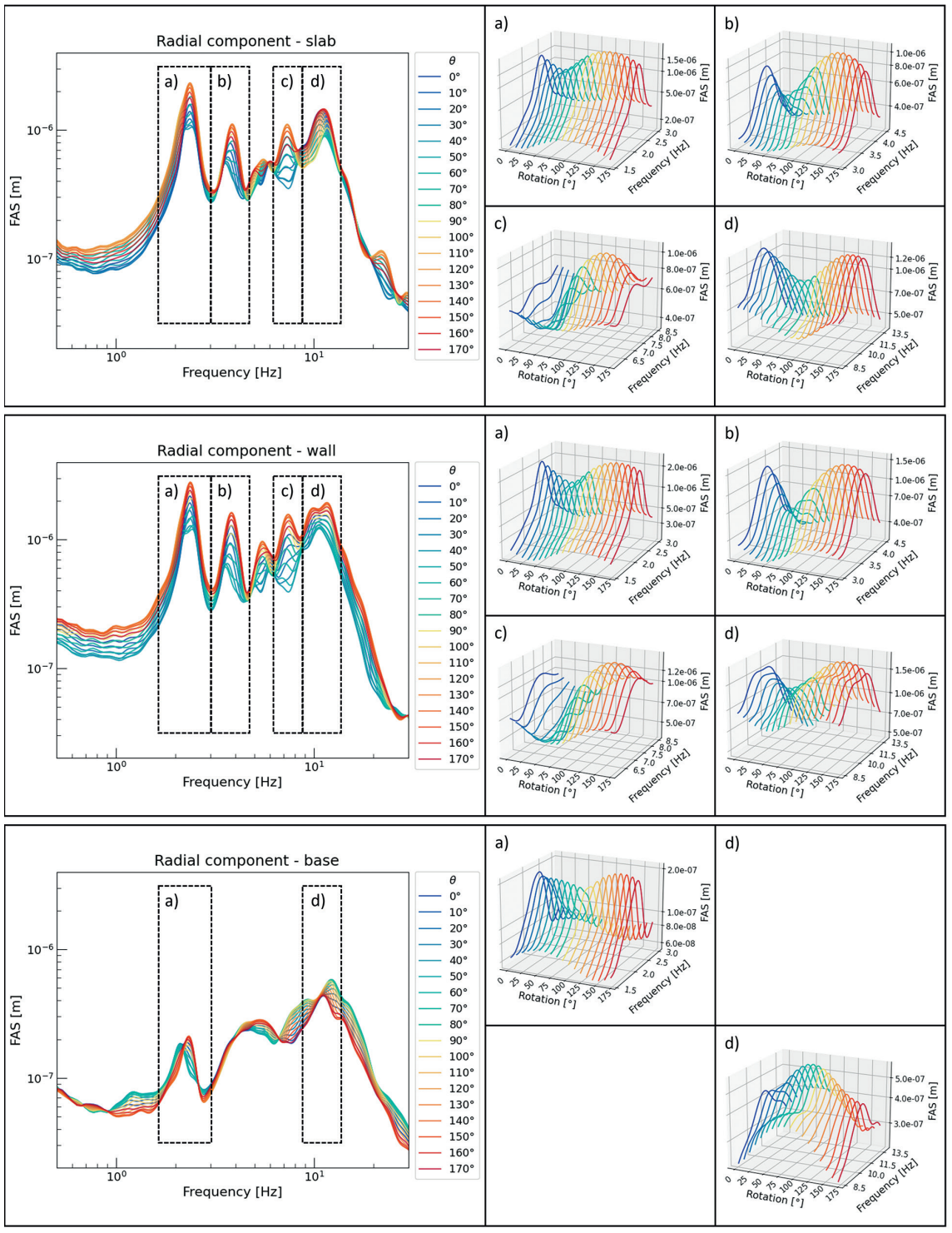

Fig. 4 - Mean *FAS*s for the radial component obtained by rotating the original signal by an angle $\theta \in [0°,180°]$ for each location (top: slab, middle: wall, bottom: base). Details of the main peaks, labelled with the letters a to d, are shown on the right.

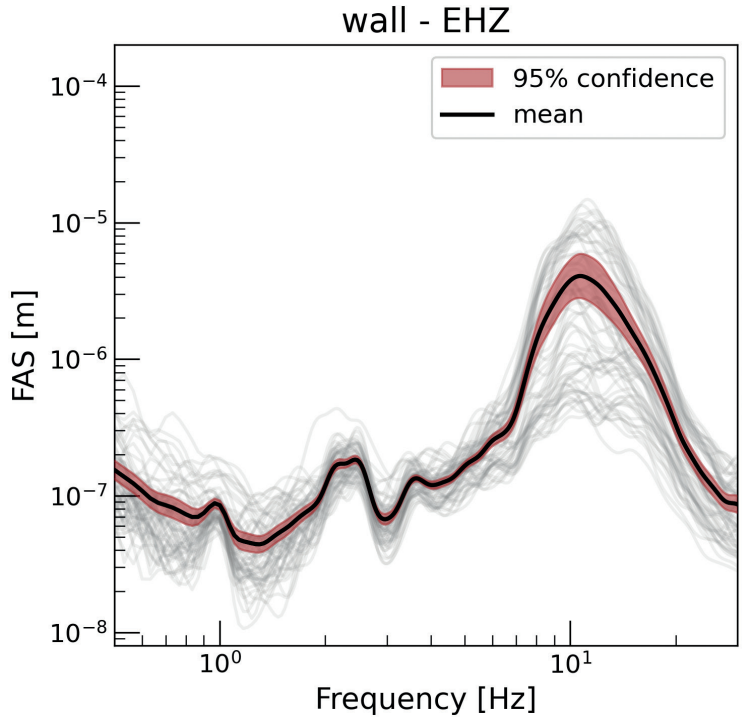

Fig. 5 - *FAS*s for the EHZ (vertical component) component of the wall site. The grey lines are the spectra for each of the 30-second windows, the thick black line is their mean, and the red shaded area is the corresponding 95% confidence interval.

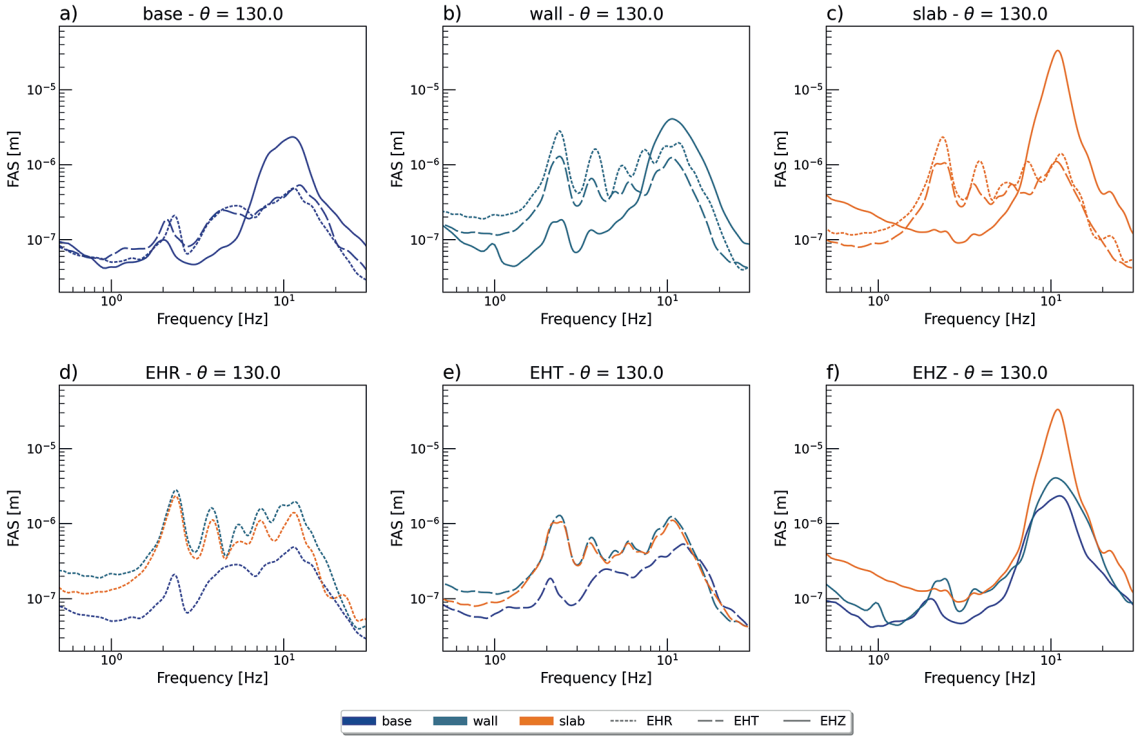

Fig. 6 - Mean *FAS*s for each site (a, b, c) and component (d, e, f). Blue, light blue, and orange lines are used for the base, wall, and slab sites, respectively. Dotted, dashed, and solid lines represent the radial, transverse, and vertical components, respectively.

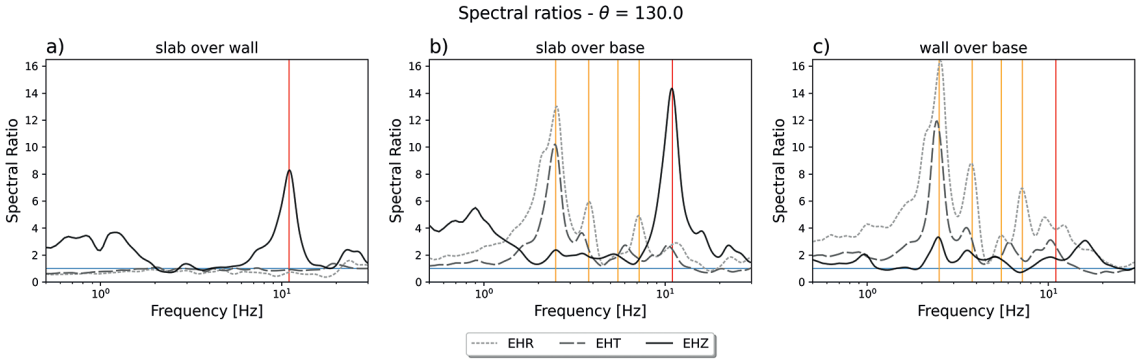

Fig. 7 - Spectral ratios for the slab/wall (a), slab/base (b), and wall/base (c) cases. The dotted, dashed, and solid lines represent the radial, transverse, and vertical components, respectively. The horizontal light blue line marks the value of the unit ratio. The vertical red line marks the peak at 11 Hz visible on the vertical components, while the vertical orange lines mark the peaks at 2.5, 3.8, 5.5, and 7.2 Hz which are visible in the ratios made with respect to the base.

the horizontal and vertical motion components. This approach is particularly useful for non-invasive seismic site characterisation and enables the identification of resonance phenomena associated with soft sedimentary layers. For this study, a 30-minute time window of ambient seismic noise was recorded at ground level, directly in front of the building, under low-noise conditions in the early morning so as to minimise interference from anthropogenic activities. Data processing was, then, performed using the hvsrpy Python-based software (Vantassel, 2024, 2025), which follows the SESAME workflow. After an initial pre-processing phase in which the raw seismic data were filtered to remove low-quality segments, spectral analysis was performed by calculating and smoothing the Fourier spectra of the three components of motion (N-S, E-W, and vertical). Subsequently, the *HVSR* curve was obtained by calculating the spectral ratio between the geometric mean of the horizontal components and the vertical component, enabling the identification of the fundamental resonance frequency from the main peak of the curve. The results of the *HVSR* analysis, including the estimated fundamental frequency of 4.2 Hz and its confidence interval, are visually represented in Fig. 8, and provide key input parameters for assessing the local seismic response, an essential step in understanding the potential dynamic interaction between soil and structure.

5. Discussion

5.1. Horizontal-to-vertical spectral ratio analysis

The *HVSR* analysis shows a primary peak at about 4.2 Hz, which is the fundamental resonance frequency of the site. This value is directly related to the local subsurface seismic response and reflects the phenomenon of seismic wave amplification at the surface in response to excitation by ambient seismic noise. The presence of a pronounced peak in this frequency range indicates a significant impedance contrast between the surface sediments and the underlying substrate, suggesting that the site is characterised by a relatively soft sedimentary layer overlying a more rigid and more compact layer. The amplitude of the primary peak is relatively high, indicating a strong local amplification of the horizontal component of the seismic waves. This phenomenon is typical for sites with a strong sedimentary cover, where the impedance contrast between the

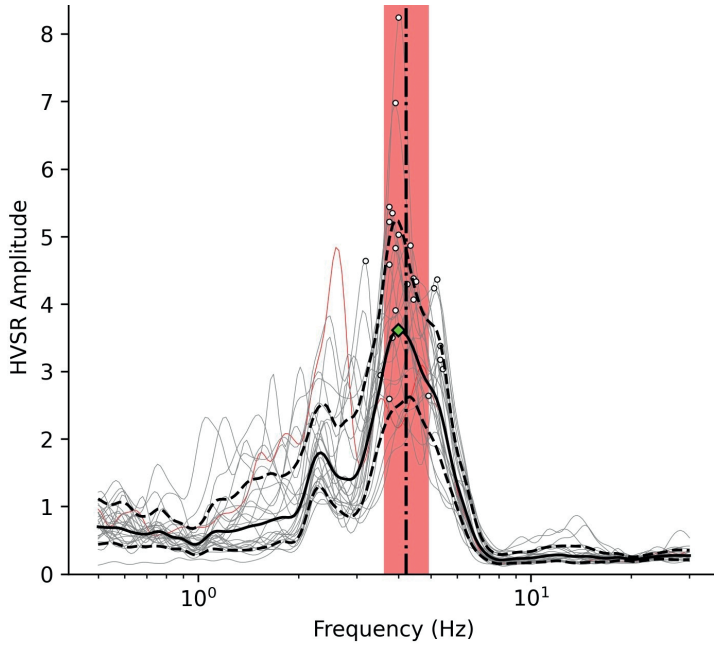

Fig. 8 - The results of the *HVSR* analysis of the background noise recorded near the building. The thick black curve represents the average spectral ratio, while the thin grey lines indicate the individual *HVSR* curves calculated for each analysis window. The curves highlighted in red correspond to the data segments discarded by the procedure. The shaded red band represents the one standard deviation range around the estimated fundamental frequency at 4.2 Hz, indicated by the black dashed vertical line.

unconsolidated sediments and the underlying substrate leads to high-energy reflection. The identification of such a well-defined peak represents a fundamental element for the dynamic characterisation of the site and enables a more accurate estimation of the depth of the rigid substrate by surface wave propagation models. In addition to the primary peak, a secondary less pronounced peak, around 2 Hz, is observed. This additional signal can be attributed to the interaction between the soil response and the dynamic properties of the structure. The presence of a building near the measurement station can introduce vibrational effects that influence the recording of ambient signals, modifying the spectral distribution of seismic energy. In particular, mid-rise buildings tend to have their own resonance frequencies between 1 and 3 Hz, and the dynamic coupling between the ground and the structure can lead to an anomaly in the spectral response, causing a secondary peak in the *HVSR* curve.

The results obtained in this study are consistent with previous research by Fitzko *et al.* (2007), who analysed site effects in the historic centre of Trieste. Their study emphasised the influence of local stratigraphy on seismic amplification, especially in areas built over thick sedimentary deposits. Their spectral analyses on another historical building, Palazzo Carciotti, revealed a dominant amplification at about 2 Hz, attributed to the resonance of the sediment layer, with secondary peaks in the range of 4-7 Hz, probably related to the dynamic response of the structure itself. The difference in the fundamental period value of the soil could be due to differences in the local stratigraphy, with a thinner sediment layer or greater stiffness of the material overlying the substrate. Furthermore, the influence of buildings on the seismic response is evident in both studies. These results emphasise the need to distinguish between pure site effects and structural interactions when interpreting the *HVSR* curves. Overall, the comparison with Fitzko *et al.* (2007)

emphasises the importance of combining different spectral analysis techniques to obtain a more comprehensive understanding of site effects. While *HVSR* provides valuable information on the fundamental resonance characteristics of a site, integration with other techniques such as standard spectral ratio or additional reference station data can refine interpretation and enable better discrimination between soil and structural contributions.

5.2. FAS and spectral ratios

Although more comprehensive analyses such as structural modelling and deconvolution would be required to fully characterise the building's vibration modes, some preliminary information can be derived from the spectral shapes and ratios. The mean *FAS* results for the wall and slab sites show a clear, well-defined peak with a frequency of 2.5 Hz (Figs. 6b and 6c), which can be interpreted as the first vibration mode of the building. The same vibration mode can also be observed in the radial component registered at the base. Considering the complexity of the structure, the following peaks at 3.8, 5.5, and 7.2 Hz could be related to higher vibration modes, as none of them coincide with the fundamental frequency of the soil, which was evaluated at 4.2 Hz in the *HVSR* noise analysis. This hypothesis is also supported by the wall/base and slab/base spectral ratios, where the presence of high peaks on the horizontal components at the considered frequencies (vertical orange lines in Figs. 7b and 7c) indicates the absence of these modes from the ground motion. This is particularly evident for the first two modes at frequencies 2.5 Hz and 3.8 Hz. A common feature of all spectra, regardless of component or location, is the peak at 11 Hz. This is particularly pronounced in vertical components (Fig. 6f), but is also present in horizontal ones. It is interesting to note that the same frequency appears to be the resonant frequency of the wooden slab. This can be clearly seen in the slab/wall spectral relationship, where the only noticeable amplification of the slab movement relative to the wall is the feature at 11 Hz in the vertical component (vertical red line in Fig. 7a). This is even more evident in the relationship between the slab and the base, which shows a strong amplification of the vertical vibration of the slab compared to the base (vertical red line in Fig. 7b). The strong amplification on the vertical motion of the slab can be attributed to the high elasticity of the wooden slab itself (located on the upper floor of the building), which can exhibit greater flexibility, due to its lower density and stiffness, compared to other construction materials (Aloisio *et al.*, 2023). This partly explains the stronger perception of the vibrations by the occupants of this floor. In addition, the possible resonance with the forcing frequency of the traffic noise can amplify the slab vibrations.

The predominant frequencies of traffic-induced ground motion were observed by Hunaidi *et al.* (2000) in the range of 5-25 Hz and by Hao *et al.* (2001) in the range of 10-20 Hz, which they interpreted as being caused by vehicle wheel-hopping. This could also be the case for bus-induced vibrations, whose predominant frequencies are known to fall within the narrower range of 10-12.5 Hz (Al-Hunaidi *et al.*, 1995). To test this hypothesis, in the following section, a disaggregation analysis is performed on the signals to separately investigate the spectral characteristics of background and vehicle noise.

5.3. Noise disaggregation

The resonance frequency at 11 Hz, observed in all components and especially in the vertical movement of the upper wooden slab, could be related to the specific excitation frequency band of the main noise source, i.e. vehicle traffic. The spectral characteristics of the noise caused specifically by vehicles passing in the vicinity can be determined by separating it from

the background noise. As described in Section 3, the building is located close to a major urban transportation hub with a steady flow of traffic throughout the day, composed of many different noise sources (from pedestrians and bicycles to motorcycles, cars, buses, vans, and trucks; there is also a railway station a few hundred metres away). As the measurements were carried out during the day and no visual recording of the traffic in the opposite streets was available, it was not possible to accurately detect every passing vehicle or overlapping of vehicles. Therefore, a classification was based on a threshold chosen as the average of the absolute value of the noise waveforms at each location. Any signals with an amplitude above the threshold, likely associated with the passage of vehicles of higher speed and mass, were, thus, separated from the background noise, which could also contain traffic contributions from more distant or lighter vehicles. Although this separation does not allow the precise identification of individual noise sources, it does allow the frequency content of the main noise contributions to be characterised. For each location, all 30-second windows, in which at least 15% of the signal values were above the threshold, were used to calculate the corresponding mean spectrum (red lines in Figs. 9 and 10), while all other windows were considered as background noise (blue lines in Figs. 9 and 10).

The results can also be compared with selected individual spectra of bus passes observed by the operators and recorded on the slab in a time window immediately after the one used for the analyses (cyan lines in Fig. 10). The bus pass-by spectra show a good agreement with the analysed spectra above the threshold, supporting the hypothesis that the buses are the main noise source for the recordings above the threshold. This feature can be taken into consideration when processing data from seismic stations in similar urban areas, should the need arise to analyse seismic recordings (including seismic noise) without the traffic noise contribution. In such cases, a machine learning algorithm can be used to separate the traffic noise from the records based on the different spectral content, as in Ertuncay *et al.* (2024).

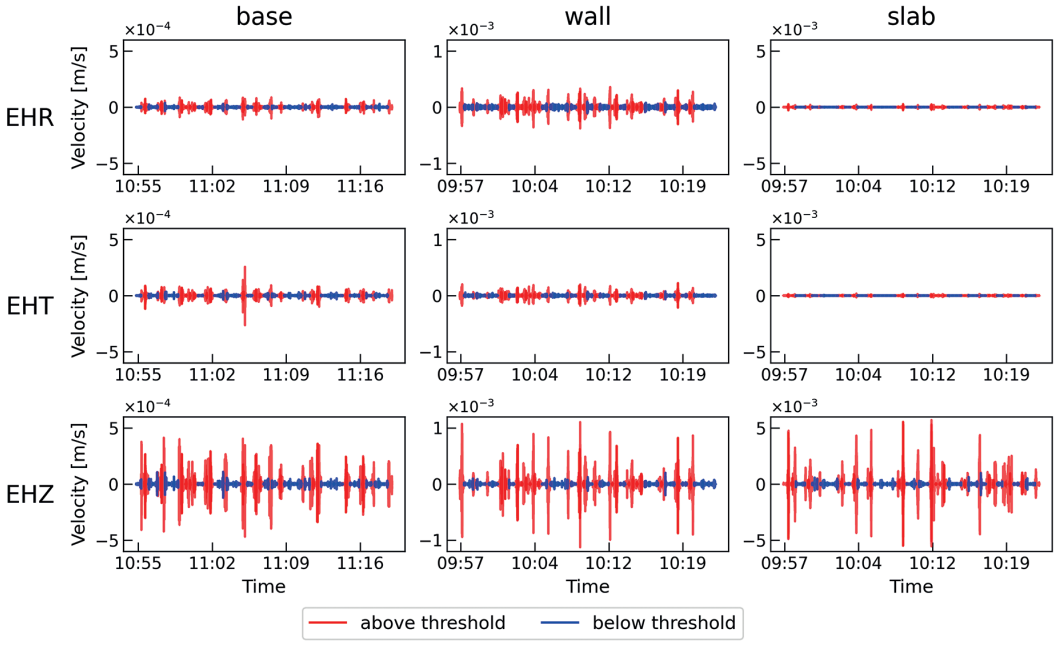

Fig. 9 - Disaggregation of the recordings at each site for all components: EHR (radial), EHT (transverse), and EHZ (vertical). The recordings are separated into windows above the threshold (red lines) and below the threshold (blue lines). The threshold value was defined as the average of the absolute value of the entire signal at each site.

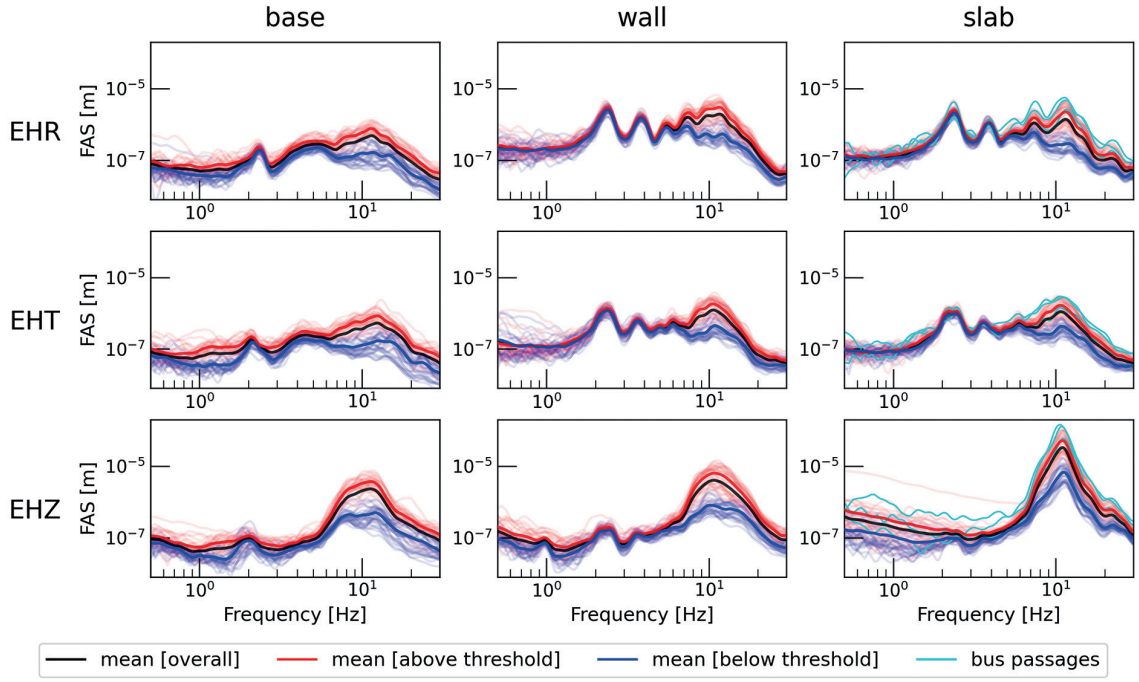

Fig. 10 - Spectra of the disaggregated recordings at each site, for all components. The red lines represent windows above the threshold; the blue lines represent windows below the threshold; the respective mean curves are shown as thick lines with the same colour code. The overall mean value is shown as a thick black line. In the case of the slab, the spectra corresponding to specific bus crossings are shown in cyan.

5.4. Occupant discomfort conditions

Internationally, there are a number of standard guidelines (e.g. national codes by the U.S. Office of Surface Mining, German Institute of Standards, and British Standards Institutions) that specify limiting values of vibrations corresponding to non-structural and structural damage levels in buildings. Most of these standards define the velocity, expressed in terms of peak particle velocity (*PPV*), as a reference damage indicator. Regarding the impact of traffic-induced vibrations on building occupants, there are numerous studies in literature dealing with the development of standards for their estimation and analysis (Hao *et al.* 2001; Beben *et al.* 2022). Athanasopoulos and Pelekis (2000) provide an overview of the thresholds related to the different levels of human discomfort for the case of continuous vibrations. The same authors also point out that floor vibration criteria alone are not able to fully predict the actual discomfort of the occupants, as the individual response of the building may lead to an increase in vibration amplitude at higher floors. The values proposed in Athanasopoulos and Pelekis (2000), therefore, refer to vibration intensities measured at the surface of inhabited building floors.

The measured *PPV* values are reported in Table 2. For comparison, the range of observed *PPV* values reported in the review by Zini *et al.* (2022) for a set of cultural heritage buildings worldwide is between 0.05 and 2.7 mm/s. In our case, we find that the *PPV* values recorded at the floor measurement points (base, wall) fall within the same range, while the *PPV* observed in the middle of the slab is significantly higher (5.71 mm/s). Although road traffic vibrations are a transient phenomenon, the high traffic concentration in the immediate vicinity of the building and the repeated and seamless bus passings may cause stacking, resulting in an

Table 2 - *PPV* values observed at the three recording sites separately considering time windows above and below the threshold.

Recording site	*PPV* [mm/s]	
	Below the threshold	Above the threshold
base	0.12	0.47
wall	0.20	1.13
slab	0.99	5.71

amplified perception of the phenomenon by the inhabitants of the highest floors. A qualitative comparison between the steady-state thresholds of Athanasopoulos and Pelekis (2000) and the vertical *PPV* values recorded on the slab and on the ground floor is shown in Fig. 11. The peak values observed on the slab, and especially those related to the bus passings (red triangles in Fig. 11), fall above the perception thresholds regardless of whether the noise is considered as steady state or transient. Even without considering the stacking effects and considering only the vibrations caused by a single bus (fully transient case), the corresponding *PPV* approaches the 'distinctly perceptible' level. The reliability of these classifications is confirmed by the complaints expressed by the occupants of the highest floor. During the installation of the instrumental deployment, we have experienced similar discomfort levels due to the vibrations of the slab. The overlap of the main frequency of the wooden slab with a higher resonance frequency of the building can, thus, be identified as the cause of the extreme amplification perceived by the occupants of the floor.

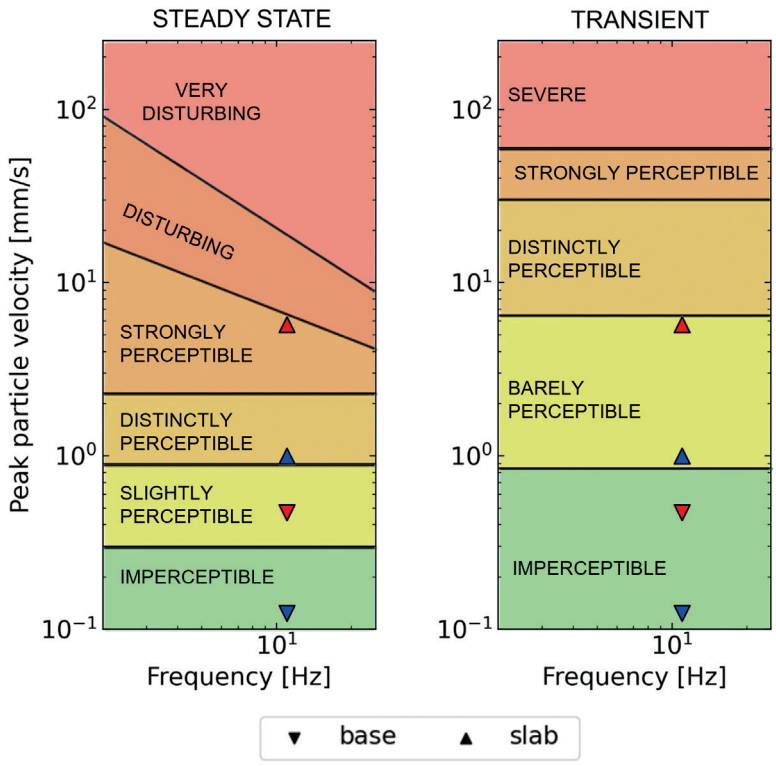

Fig. 11 - Threshold vibration criteria as reported by Athanasopoulos and Pelekis (2000) corresponding to different levels of human discomfort expressed in terms of *PPV*. The *PPV* values obtained in this study for the slab floor (triangles) and for the base floor (reversed triangles) are reported for comparison, in red for signals above the threshold (corresponding to heavy bus traffic) and in blue for signals below the threshold.

5.5. Implications and further developments

The use of cost-effective sensors provides a relatively fast and non-invasive method that can easily be applied to multiple buildings in urban areas. Ambient noise measurements have proven to be effective in characterising vibrations and determining their origin, as they represent a standardised and easily reproducible method. However, the method could be complemented by modelling building behaviour (Erkal *et al.*, 2020). The results of this study can support the identification of potential mitigation measures, such as road pavement improvement and diversion of heavy road traffic, which might effectively mitigate the discomfort caused by traffic-induced vibrations. Solutions to reduce the impact of vibrations may include interventions in the road infrastructure. In addition, a revision of the circulating vehicle types allowed access and heavy-traffic routes could limit the exposure of the most vulnerable buildings to vibrations and related inconveniences. A combination of these measures could effectively reduce the inconvenience caused by traffic-induced vibrations. The approach used in this study demonstrates the potential of rapid survey with cost-effective instruments for assessing the impact of traffic-induced vibrations on buildings and illustrates the possibility of application in different contexts. This aspect is particularly advantageous for integration into urban seismic monitoring networks, which are becoming increasingly dense (Scudero *et al.*, 2023; Bragato *et al.*, 2025). For urban planning applications, the proposed methodology is equally valuable as the obtained measurements can support urban redevelopment by providing important data for the planning of vibration mitigation measures at structural and infrastructural level, thus, improving the environmental quality in urban areas (Simone *et al.*, 2008; Vuye *et al.*, 2016).

The analysis carried out makes it clear that further developments are needed to refine the understanding of the phenomenon and improve mitigation strategies. An important aspect is the enhanced characterisation of buildings, which could be achieved through advanced structural modelling or by applying more sophisticated techniques such as deconvolution or frequency-domain decomposition that require the deployment of a denser sensor array. The integration of experimental measurements and numerical modelling represents a promising way to improve urban vibration management, ensuring a balance between the needs of infrastructure development and the preservation of built heritage. Another promising development is the extension of these techniques to the urban scale, implementing continuous monitoring of traffic impact in historic cities.

6. Conclusions

The study carried out an in-depth analysis of the effects of traffic-induced vibrations on a historic building, in the Borgo Teresiano district of Trieste, and showed how such phenomena can affect residents. The analysis showed that the vibrations caused by the passage of heavy vehicles, particularly urban buses, can be amplified by the combination of the dynamic characteristics of the structure and the geotechnical characteristics of the subsoil. Thanks to the use of cost-effective sensors, the resonant frequencies of the building could be determined quickly and non-invasively, enabling a better understanding of the relationship between traffic and structural response. The results show that:

1. the first vibration mode of the building is around 2.5 Hz, while higher vibration modes occur between 3.8 Hz and 7.2 Hz; none of these peaks seem to overlap with the fundamental frequency of the soil estimated at 4.2 Hz;

2. the peak detected at 11 Hz, which is particularly evident in the vertical movement of the upper wooden floor, is consistent with the characteristic frequencies associated with heavy traffic noise, suggesting that the repeated passing of buses may produce an amplified resonance effect that is particularly noticeable on the upper floors of the building;
3. the analysis of the vibrations perceived by the residents confirmed that the recorded values exceed the perception thresholds defined in the literature, in particular according to the studies by Athanasopoulos and Pelekis (2000). The observed maximum particle velocities are in a range that is perceived as disturbing or even uncomfortable by the occupants of the upper floors, suggesting that the elasticity of the wooden floor adds to the sensation of discomfort.

We can conclude that heavy traffic affects the residents of historical buildings typical of the study area, in particular in case of wooden floors which have a strong elastic behaviour. Ambient noise measurements can, therefore, be used as a preliminary screening tool before performing more sophisticated analyses on building expected response, or prior to assessing potential mitigation measures.

Acknowledgements. Figures were made with Matplotlib version 3.8.4 (Hunter, 2007), and the Matplotlib Development Team, available under the Matplotlib license at https://matplotlib.org/. Software packages from ObsPy (Beyreuther *et al.*, 2010) were used for data analysis, including the computation of the *HVSR* curve, the latter performed using hvsrpy, the Python-based software (Vantassel, 2024, 2025).The dataset for this monitoring experiment is provided in Capotosti *et al.* (2025) and includes both raw (uncorrected) and instrument-corrected seismic recordings acquired with the Lunitek Sentinel GEO sensor in four configurations: at the base of the building, on the top-wall, on the top-slab, and at a nearby free-field site. All recordings are provided in MiniSEED format, together with StationXML metadata and computation of the HVSR curve, the latter performed using hvsrpy, the Python-based software (Vantassel, 2024, 2025).

REFERENCES

Al-Hunaidi M.O., Rainer J.H., Pernica G. and Tremblay M.; 1995: *Traffic-induced vibration in buildings - Use of site cut-off frequency as a remedial measure.* WIT Trans. The Built Environ., 15, 10, doi: 10.2495/SD950621.

Aloisio A., Pasca D.P., De Santis Y., Hillberger T., Giordano P.F., Rosso M.M., Tomasi R., Limongelli M.P. and Bedon C.; 2023: *Vibration issues in timber structures: a state-of-the-art review.* J. Build. Eng., 76, 107098, doi: 10.1016/j.jobe.2023.107098.

ANC (Association of Noise Consultants); 2012: *Measurement and assessment of ground-borne noise and vibration*. (ANC Guidelines), <www.association-of-noise-consultants.co.uk/measurement-and-assessment-of-groundborne-noise-and-vibration>.

Athanasopoulos G.A. and Pelekis P.C.; 2000: *Ground vibrations from sheetpile driving in urban environment: measurements, analysis and effects on buildings and occupants.* Soil Dyn. Earthquake Eng., 19, 317-387, doi: 10.1016/S0267-7261(00)00008-7.

Bard P.Y. (coord); 2004: *SESAME. Guidelines for the implementation of the H/V spectral ratio technique on ambient vibrations Measurements, processing, and interpretation.* European Commission, 62 pp., <https://sesame.geopsy.org/Papers/HV_User_Guidelines.pdf>.

Beben D., Maleska T., Bobra P., Duda J. and Anigacz W.; 2022: *Influence of traffic-induced vibrations on humans and residential building - a case study.* Int. J. Environ. Res. Public Health, 19, 5441, doi: 10.3390/ijerph19095441.

Beyreuther M., Barsch R., Krischer L., Megies T., Behr Y. and Wassermann J.; 2010: *ObsPy: a python toolbox for seismology.* Seismol. Res. Lett., 81, 530-533, doi: 10.1785/gssrl.81.3.530.

Bongiovanni G., Clemente P.M., Rinaldis D. and Saitta F.; 2011: *Traffic-induced vibrations in historical buildings*. In: Proc. of the 8th Int. Conf. Struct. Dyn., EURODYN 2011, Leuven, Belgium.

Bragato P.L., Boaga J., Capotosti G., Comelli P., Parolai S., Rossi G., Siracusa H., Zian P. and Zuliani D.; 2025: *Implementing a dense accelerometer network in Veneto (NE Italy): a support for rapid earthquake impact assessment.* Bull. Earthquake Eng., 23, 1859-1884, doi: 10.1007/s10518-025-02133-w.

BSI (British Standards Institution); 2008: *Guide to evaluation of human exposure to vibration in buildings (1 Hz to 80 Hz) - Part 1: vibration sources other than blasting (BSI Standard No. 6472:2008).* <knowledge.bsigroup.com/products/guide-to-evaluation-of-human-exposure-to-vibration-in-buildings-vibration-sources-other-than-blasting>.

Busetti M., Zgur F., Romeo R., Sormani L. and Pettenati F.; 2012: *Caratteristiche geologico-strutturali nel Golfo di Trieste.* In: D'Angelo S. and Fiorentino A. (eds),Contributi al meeting marino 25-26 ottobre 2012, Atti ISPRA, Roma, Italy, pp. 65-70.

Caballol D., Rapaso A.P., Carrillo F.G. and Morales-Segura M.; 2022: *Measurement of ambient vibration in empty buildings and relation to external noise.* Soil Dyn. Earthquake Eng. 31, 692-707, doi: 10.1016/j.apacoust.2021.108431.

Capotosti G., Cataldi L., Ertuncay D., Scaini C. and Poggi V.; 2025: *Supplements to: the assessment of the traffic-induced vibrations in urban areas by cost-effective sensors: a case study for a historic building in Trieste, north-eastern Italy.* Dataset Zenodo, doi: 10.5281/zenodo.15297034.

Celebi M.; 2000: *Seismic instrumentation of buildings (with emphasis on federal buildings).* USGS Open-File Report, 2000-157, 37 pp., doi: 10.3133/ofr00157.

Costanzo A., Falcone S., La Piana C., Lapenta V., Musacchio M., Sgamellotti A. and Buongiorno M.F.; 2022a: *Traffic-induced vibrations on cultural heritage in urban area: the case of Villa Farnesina in Rome.* J. Phys.: Conf. Ser., 2204, 012043, doi: 10.1088/1742-6596/2204/1/012043.

Costanzo A., Falcone S., La Piana C., Lapenta V., Musacchio M., Sgamellotti A. and Buongiorno M.F.; 2022b: *Laser scanning investigation and geophysical monitoring to characterise cultural heritage current state and threat by traffic-induce vibrations: the Villa Farnesina in Rome.* Rem. Sens., 14, doi: 10.3390/rs14225818.

Crispino M. and D'Apuzzo M.; 2001: *Measurement and prediction of traffic-induced vibrations in a heritage building.* J. Sound Vibr., 246, 319-335, doi: 10.1006/jsvi.2001.3648.

Erkal A. and Kocagöz M.S.; 2020: *Interaction of vibrations of road and rail traffic with buildings and surrounding environment.* J. Perform. Constr. Facil., 34, 04020038, doi: 10.1061/%28ASCE%29CF.1943-5509.0001442.

Erkal A., Laefer D., Fanning P., Durukal E., Hancilar U. and Kaya Y.; 2010: *Factors affecting traffic-generated vibrations on structures and the masonry minaret of Little Hagia Sophia*. In: Joint Symp. Proc. Bridge and Concr. Res., Ireland, Cork, Ireland, <hdl.handle.net/10197/4870>.

Ertuncay D., De Lorenzo A. and Costa G.; 2024: *Deep learning based earthquake and vehicle detection algorithm*. J. Seismol., 29, 269-281, doi: 10.1007/s10950-024-10267-8.

Fitzko F., Costa G., Delise A. and Suhadolc P.; 2007: *Site effects analyses in the old city center of Trieste (NE Italy) using accelerometric data.* J. Earthquake Eng., 11, 33-48, doi: 10.1080/13632460601123123.

Gallipoli M.R., Mucciarelli M. and Vona M.; 2009: *Empirical estimate of fundamental frequencies and damping for Italian buildings*. Earthquake Eng. Struct. Dyn., 38, 973-988, doi: 10.1002/eqe.878.

Gallipoli M.R., Petrovic B., Calamita G., Tragni N., Scaini C., Barnaba C., Vona M. and Parolai S.; 2023: *Towards specific T-H relationships: FRIBAS database for better characterization of RC and URM buildings.* Bull. Earthquake Eng., 21, 2281-2307, doi: 10.1007/s10518-022-01594-7.

Gordini E., Caressa S. and Marocco R.; 2003: *New morpho-sedimentological map of Trieste Gulf (from Punta Tagliamento to Isonzo mouth)*. Gortania, Atti del Museo Friulano di Storia Naturale, 25, 5-29.

Guillier B., Chatelain J.L., Perfettini H., Oubaiche E.H., Voisin C., Bensalem R., Machane D. and Hellel M.; 2016: *Building frequency fluctuations from continuous monitoring of ambient vibrations and their relationship to temperature variations*. Bull. Earthquake Eng., 14, 2213-2227, doi: 10.1007/s10518-016-9901-z.

Hao H., Ang T.C. and Shen J.; 2001: *Building vibration to traffic-induced ground motion.* Build. Environ., 36, 321-336, doi: 10.1016/S0360-1323(00)00010-X.

Hunaidi O., Guan W. and Nicks J.; 2000: *Building vibrations and dynamic pavement loads induced by transit buses.* Soil Dyn. Earthquake Eng., 19, 435-453, doi: 10.1016/S0267-7261(00)00019-1.

Hunter J.D.; 2007: *Matplotlib: a 2D graphics environment.* Comput. Sci. & Eng., 9, 90-95, doi: 10.1109/MCSE.2007.55.

ISO (International Organization for Standardization); 2003: *Mechanical vibration and shock - evaluation of human exposure to whole-body vibration - Part 2: Vibration in buildings (1 Hz to 80 Hz).* ISO Standard No. 2631-2:2003, <www.iso.org/standard/23012.html>.

Konno K. and Ohmachi T.; 1998: *Ground-motion characteristics estimated from spectral ratio between horizontal and vertical components of microtremor.* Bull. Seismol. Soc. Am., 88, 228-241, doi: 10.1785/BSSA0880010228.

Kouroussis G., Verlinden O. and Conti C.; 2011: *Free field vibrations caused by high-speed lines: measurement and time domain simulation.* Soil Dyn. Earthquake Eng., 31, 692-707, doi: 10.1016/j.soildyn.2010.11.012.

Lopes P., Ruiz J.F., Costa P.A., Rodríguez L.M. and Cardoso A.S.; 2016: *Vibrations inside buildings due to subway railway traffic. Experimental validation of a comprehensive prediction model.* Sci. The Total Environ., 568, 1333-1343, doi: 10.1016/j.scitotenv.2015.11.016.

Meli R., Faccioli E., Murià-Vila D., Quaas R. and Paolucci R.; 1998: *A study of site effects and seismic response of an instrumented building in Mexico City.* J. Earthquake Eng., 2, 89-111, doi: 10.1080/13632469809350315.

Mucciarelli M. and Gallipoli M.R.; 2007: *Non-parametric analysis of a single seismometric recording to obtain building dynamic parameters.* Ann. Geophys., 50, 259-266, doi: 10.4401/ag-3079.

Mugnai F., Caporossi P. and Mazzanti P.; 2022: *Exploiting image assisted total station in digital image correlation (DIC) displacement measurements: insights from laboratory experiments.* Eur. J. Rem. Sens., 55, 115-128, doi: 10.1080/22797254.2021.2025153.

Nakamura Y.; 1989: *A method for dynamic characteristics estimation of subsurface using microtremor on the ground surface.* Railway Tech. Res. Inst., 30, 25-33.

Nakamura Y.; 1996: *Research and development of intelligent earthquake disaster prevention systems UrEDAS and HERAS.* Journal of Structural Mechanics and Earthquake Engineering, 531, 1-33.

Nakamura Y.; 2000: *Clear identification of fundamental idea of Nakamura's technique and its applications.* In: 12th World Conf. on Earthquake Eng., Auckland, New Zealand, Paper 2656, 8 pp.

Olsson U.; 2005: *Confidence intervals for the mean of a log-normal distribution.* J. Stat. Educ., 13, doi: 10.1080/10691898.2005.11910638.

Paolucci R.; 1993: *Soil-structure interaction effects on an instrumented building in Mexico City.* Eur. Earthquake Eng., 3, 33-44.

Petrovic B., Scaini C. and Parolai S.; 2023: *The damage assessment for rapid response (DARR) method and its application to different ground-motion levels and building types.* Seismol. Res. Lett., 94, 1536-1555, doi: 10.1785/0220210350.

Pridham B., Normile T., Kronenwetter C., Reynolds P. and Hudson E.; 2021: *Control of traffic-induced ground vibrations in a residential structure.* Dyn. Civil Struct., 2, 251-259, doi: 10.1007/978-3-030-47634-2_29.

Regione Autonoma Friuli Venezia Giulia - Comune di Trieste; 2016a: *Microzonazione sismica - relazione illustrativa*. <documenti.online.trieste.it/edilizia/prg/MZS/Relazione_illustrativa_MS1_Trieste.pdf>.

Regione Autonoma Friuli Venezia Giulia - Comune di Trieste; 2016b: *Carta delle MOPS Tav. 3*. <documenti.online.trieste.it/edilizia/prg/MZS/Carta_delle_MOPS_Tavola_3.pdf>.

Rivas J., Wunderlich R. and Heinen S.J; 2012: *A MEMS acceleration sensor for traffic condition detection.* In: 8th Conference on Ph.D. Research in Microelectronics & Electronics, PRIME 2012, Aachen, Germany, 2012, pp. 1-4.

Scaini C., Petrovic B., Tamaro A., Moratto L. and Parolai S.; 2021: *Near-real-time damage estimation for buildings based on strong motion recordings: an application to target areas in northeastern Italy.* Seismol. Res. Lett., 92, 3785-3800, doi: 10.1785/0220200430.

Scudero S., Costanzo A. and D'Alessandro A.; 2023: *Urban seismic networks: a worldwide review.* Appl. Sci., 13, 13165, doi: 10.3390/app132413165.

Shiferaw H.M.; 2021: *Measuring traffic induced ground vibration using smartphone sensors for a first hand structural health monitoring.* Sci. Afr., 11, e00703, doi: 10.1016/j.sciaf.2021.e00703.

Sica G., Peris E., Woodcock J.S., Moorhouse A.T. and Waddington D.C.; 2014: *Design of measurement methodology for the evaluation of human exposure to vibration in residential environments.* Sci. The Total Environ., 482-483, 461-471, doi: 10.1016/j.scitotenv.2013.07.006.

Simone A., Lantieri C. and Vignali V.; 2008: *Vibrazioni da traffico in aree urbane: effetti sugli edifici e tecniche di attenuazione.* In: Atti XVII Convegno Nazionale SIIV, Le reti di trasporto urbano. Progettazione, Costruzione, Gestione, Enna, Italy.

Vantassel J.P.; 2024: *Jpvantassel/Hvsrpy: v2.0.0.* Zenodo, doi: 10.5281/zenodo.3666956.

Vantassel J.P.; 2025: *Hvsrpy: an open-source python package for microtremor and earthquake horizontal-to-vertical spectral ratio processing.* Seismol. Res. Lett., 96, 2671-2682, doi: 10.1785/0220240395.

Vuye C., Musovic F., Tyszka L., Van den Bergh W., Kampen J., Bergiers A., Maeck J., Buytaert A. and Vanhooreweder B.; 2016: *First experiences with thin noise reducing asphalt layers in an urban environment in Belgium.* In: Proc. ISMA2016 Int. Conf. on Noise and Vibration Engineering and USD2016 Int. Conf. on Uncertainty in Structural Dynamics, Belgium, pp. 81-94, <hdl.handle.net/10067/1415290151162165141>.

Waddington D.C., Woodcock J., Peris E., Condie J., Sica G., Moorhouse A.T. and Steele A.; 2014: *Human response to vibration in residential environments.* J. Acoust. Soc. Am., 135, 182-193, doi: 10.1121/1.4836496.

Woodcock J., Peris E., Condie J., Sica G., Koziel Z., Evans T., Moorhouse A., Steele A. and Waddington D.C.; 2012: *Human response to vibration in residential environments (NANR209). Tech. Rep. 6: Determination of exposure-response relationships.* Defra, London, pp. 182-193.

Zhang Y., Elita Li Y., Zhang H. and Ku T.; 2019: *Near-surface site investigation by seismic interferometry using urban traffic noise in Singapore.* Geophys., 84, B169-B180, doi: 10.1190/geo2017-0798.1.

Zini G., Betti M. and Bartoli G.; 2022: *Experimental analysis of the traffic-induced-vibration on an ancient lodge.* Struct Control Health Monit., 29, e2900, doi: 10.1002/stc.2900.

Corresponding author: Giorgio Capotosti
Center for Seismological Research
National Institute of Oceanography and Applied Geophysics – OGS
Via della Libertà 12, 30175 Marghera (VE), Italy
Phone: +39 3516099383; e-mail: gcapotosti@ogs.it

Appendix

The calculation of the mean *FAS*s and their associated uncertainty for each frequency value was carried out following the modified Cox method proposed by Olsson (2005). The starting assumption is that the *FAS* value at each frequency can be considered as a log-normally distributed variable *X*:

$$X = FAS \tag{A1}$$

$$f(X) = \frac{1}{X\sigma\sqrt{2\pi}} e^{-\frac{1}{2}\left(\frac{lnln\,X - \mu}{\sigma}\right)^2}. \tag{A2}$$

Therefore, its natural logarithm is a variable *Y* with normal distribution:

$$Y = ln(FAS) \tag{A3}$$

$$f(Y) = \frac{1}{\sigma\sqrt{2\pi}} e^{-\frac{1}{2}\left(\frac{Y - \mu}{\sigma}\right)^2}. \tag{A4}$$

The mean value ($\hat{\mu}$) and the variance of *Y* ($\hat{\sigma}^2$) can be estimated as:

$$E[Y] = \hat{\mu} = \frac{1}{n-1} \sum_i Y_i \tag{A5}$$

$$VAR[Y] = \hat{\sigma}^2 = \frac{1}{n-1} \sum_i \left(Y_i - \hat{\mu}\right)^2 \tag{A6}$$

where *n* in the number of *FAS* values at the analysed frequency.

The mean value of X ($\hat{\mu}_X$) can be subsequently estimated as:

$$E[X] = \hat{\mu}_X = e^{\hat{\mu}+\frac{1}{2}\hat{\sigma}^2}. \quad \text{(A7)}$$

The uncertainty associated with this mean value can be estimated starting from the statistical properties calculated in the logarithm scale. We can obtain the estimate of the mean of X in logarithmic scale ($lnln\hat{\mu}_X$) as:

$$E\left[lnln\,\hat{\mu}_X\right] = lnln\hat{\hat{\mu}}_X = \hat{\mu} + \frac{1}{2}\hat{\hat{\sigma}}^2 \quad \text{(A8)}$$

and the estimate of its variance as:

$$VAR\left[lnln\hat{\hat{\mu}}_X\right] = \frac{\hat{\hat{\sigma}}^2}{n} + \frac{\hat{\hat{\sigma}}^4}{2\,(n-1)}. \quad \text{(A9)}$$

The confidence interval around $lnln\hat{\mu}_X$, for example of level C = 0.95, can be thus calculated as:

$$CI\left[lnln\hat{\hat{\mu}}_X\,,\,C\right] = z_{n-1}\left(\frac{1-C}{2}\right) \bullet STD\left[lnln\hat{\hat{\mu}}_X\right] = z_{n-1}\left(\frac{1-C}{2}\right) \bullet \sqrt{\frac{\hat{\hat{\sigma}}^2}{n} + \frac{\hat{\hat{\sigma}}^4}{2\,(n-1)}} \quad \text{(A10)}$$

where $z_{n-1}\left(\frac{1-C}{2}\right)$ is the critical value of the t-Student distribution for $n-1$ degrees of freedom corresponding to an exceedance probability of $\frac{1-C}{2}$ = 0.025, and STD [$lnln\hat{\mu}_X$] is the standard deviation associated to $lnln\hat{\mu}_X$ obtained as the square root of Eq. (A9).

Finally, the C % confidence interval associated to the mean value of X at a given frequency in linear scale ($\hat{\mu}_X$) is obtained as:

$$\left[e^{\left(\hat{\mu}+\frac{1}{2}\hat{\sigma}^2\right)-CI\left[lnln\hat{\hat{\mu}}_X,\;C\right]},\; e^{\left(\hat{\mu}+\frac{1}{2}\hat{\sigma}^2\right)+CI\left[lnln\hat{\hat{\mu}}_X,\;C\right]}\right] = \left[\frac{\hat{\mu}_X}{e^{CI\left[lnln\hat{\hat{\mu}}_X,\;C\right]}},\; \hat{\mu}_X \bullet e^{CI\left[lnln\hat{\hat{\mu}}_X,\;C\right]}\right]. \quad \text{(A11)}$$